Published in final edited form as:
Cell Rep. 2014 May 8; 7(3): 859–870. doi:10.1016/j.celrep.2014.03.042.

Persistent replicative stress alters Polycomb phenotypes and tissue homeostasis in *Drosophila melanogaster*

Severine Landais[1], **Cecilia D'Alterio**[1,2], and **D. Leanne Jones**[1,2,*]

[1]Laboratory of Genetics, The Salk Institute for Biological Studies, La Jolla, CA 92037

[2]Department of Molecular, Cell, and Developmental Biology, University of California, Los Angeles, Los Angeles, CA 90095, USA

Abstract

Polycomb group (PcG) proteins establish and maintain genetic programs that regulate cell fate decisions. *Drosophila multi sex combs (mxc)* was categorized as a *PcG* gene based on a classical Polycomb phenotype and genetic interactions; however, a mechanistic connection between Polycomb and Mxc has not been elucidated. Hypomorphic alleles of *mxc* are characterized by male and female sterility and ectopic sex combs. Mxc is an important regulator of histone synthesis, and we find that increased levels of the core histone H3 in *mxc* mutants result in replicative stress and a persistent DNA damage response (DDR). Germline loss, ectopic sex combs and the DDR are suppressed by reducing H3 in *mxc* mutants. Conversely, *mxc* phenotypes are enhanced when the DDR is abrogated. Importantly, replicative stress induced by hydroxyurea treatment recapitulated *mxc* germline phenotypes. These data reveal how persistent replicative stress affects gene expression, tissue homeostasis, and maintenance of cellular identity *in vivo*.

Keywords

mxc; germline; histones; replicative stress; DNA repair; Polycomb

Introduction

Proper development and tissue homeostasis require stabilization of cell identity as well as plasticity of gene expression. The Polycomb group (PcG) proteins are chromatin modifiers that act as transcriptional repressors, which were first described in *Drosophila* more than 30 years ago. Originally, they were characterized as regulators of homeotic gene expression, such as the *Hox* genes, that pattern the anterior-posterior body plan during development (Lewis, 1978); however, since that time, PcG proteins have been demonstrated to be

*To whom correspondence should be addressed: Leanne Jones **Postal address:** University of California, Los Angeles Department of Molecular, Cell, and Developmental Biology Terasaki Life Sciences Building, Room 5139 610 Charles E. Young Dr. South Los Angeles, CA 90095 office: 310-206-7066 leannejones@ucla.edu.

conserved across species and play important roles in regulating stem cell behavior and cancer progression (Sauvageau and Sauvageau, 2010).

Two core complexes composed of canonical PcG proteins, Polycomb Repressive Complexes PRC1 and PRC2, have been described; however, the composition of PRC complexes is variable and context dependent. One role for PRC2 is methylation of histone H3 on lysine 27 to generate H3K27me3, a modification thought necessary to recruit PRC1, which can then catalyze histone H2A monoubiquitylation on lysine 119 (K118 in *Drosophila*) to strengthen gene repression (Schwartz and Pirrotta, 2007). Some proteins have been classified as PcG proteins based on association with PRC 1 or 2 (Sparmann and Lohuizen, 2006), while other genes, such as *Drosophila multi sex combs* (*mxc*), exhibit robust genetic interactions with *PcG* genes but have not been found associated with either PcG complex (Saget et al., 1998; Santamaría and Randsholt, 1995).

Hypomorphic alleles of *mxc* are characterized by hematopoietic defects, male and female sterility, and a classical *Drosophila* Polycomb phenotype consisting of ectopic sex combs (Docquier et al., 1996; Santamaria, 1995). Recently, *mxc* was found to localize to the histone locus body (HLB) and play a key role in histone synthesis (White et al., 2011). Consequently, Mxc was proposed to be the *Drosophila* equivalent of mammalian NPAT (**n**uclear **p**rotein of the **a**taxia **t**elangiectasia-mutated gene) (White et al., 2011). Although NPAT has been shown to be necessary for histone synthesis and cell cycle progression in human embryonic stem cells (Becker et al., 2010; Ghule et al., 2008), no links between defects in histone synthesis and maintenance of cell fates have been demonstrated previously. Our characterization of *mxc* phenotypes has revealed that persistent replicative stress and an ongoing DNA damage response can lead to alterations in cellular identities and a loss of tissue homeostasis, resembling disruption of Polycomb function.

Results

Mutations in *mxc* disrupt germline homeostasis

Two populations of adult stem cells reside at the tip of the *Drosophila* testis : the germline stem cells (GSCs) and somatic cyst stem cells (CySCs). GSCs and CySCs are in direct contact with a cluster of somatic cells, known as the hub, that serve as a critical component of the stem cell niche (Kiger et al., 2001; Leatherman and Dinardo, 2010; Tulina and Matunis, 2001) (Figure 1A). GSCs divide asymmetrically to generate another GSC and a gonialblast, which is displaced away from the hub and initiates differentiation by undergoing 4 rounds of mitotic, transit amplification (TA) divisions with incomplete cytokinesis, to generate a cyst of 16 interconnected spermatogonia. After pre-meiotic S phase, spermatogonia increase in volume approximately 25 times, differentiate into spermatocytes, and undergo meiosis to generate mature, haploid sperm (Figure 1A, B) (Fuller, 1993).

Although the effects of the *mxc* mutation are not specific to germ cells, the weakest, viable allele of *mxc*, mxc^{G46}, distinguishes itself by having a dramatic germ line phenotype (Figures 1C and S1A). An *mxc::GFP* transgene completely rescued lethality of animals carrying the strongest *mxc* alleles, as well as the germline defects present in mxc^{G46} mutant males (Figure 1D). Consistent with previous results, Mxc localized to discrete subnuclear

foci in all cells throughout the testis, corresponding to the histone locus body (HLB) (White et al., 2011) (Figure S1B-C). Tissue homeostasis is severely compromised in testes from mxc^{G46} mutants, with loss of germ cells and disruption of the normal spatiotemporal gradient of germ cell development and differentiation (Figure 1B, C). A detailed characterization of the effect of mxc^{G46} mutations on the adult male germ line revealed three distinct phenotypes: 1) testes containing disorganized spermatogonia and larger germ cells harboring characteristics of mature spermatocytes (Figure 1F), 2) testes containing only spermatogonia (Figure 1G), and 3) complete loss of the germ line, with clusters of somatic cyst cells adjacent to the hub (Figure 1H). Over time, the percentage of testes with complete loss of the germ line increased significantly (Figure 1I).

Somatic cyst cells strongly influence the behavior of GSCs and spermatogonial differentiation; therefore, *mxc* function could be required in germ cells, somatic cells, or both, resulting in the observed germline defects in *mxc* mutant males. In order to determine whether *mxc* acts cell-autonomously to regulate GSC maintenance, FRT-mediated clonal analysis was used to generate germ cells that were homozygous mutant for the null mxc^{G48} allele (Figure S1A) (see Materials and Methods for details) (Xu and Rubin, 1993). In comparison to mxc^{+} GSCs, significantly fewer mxc^{G48} mutant GSCs were maintained over time (Figure 1J-L), suggesting that *mxc* acts autonomously in the germ line to regulate maintenance of GSCs. This is consistent with the loss of GSCs in newly eclosed (hatched) 1-day old (1 do) *mxc* mutant males [control (*w*-): 9.9±2.5 s.d. (n=16); mxc^{G46}/Y: 6.2±2.0 (n=18); mxc^{G43}/Y: 4.1±3.3 (n=18).]

Importantly, the loss of germ cells in *mxc* mutant males is not due to an inability to undergo cell division, as *mxc* mutant spermatogonial cysts were observed frequently (Figure S1D). Furthermore, in newly eclosed mxc^{G46} males, large germ cells in groups of <16 are observed that express markers of differentiation, such as the spermatocyte marker *cannonball* (*can*) (Figure 1C, 1F, 1M and 1N). Thus, early germ cells appear to undergo mitosis but initiate a terminal differentiation program before completion of the four TA divisions. Furthermore, germ cells in testes from mxc^{G46} males incorporate EdU, a thymidine analog, indicating that cells continue to proliferate and progress through S-phase. However, EdU^{+} germ cells begin to accumulate throughout the testis in 5 and 10do mxc^{G46} males, suggesting that these germ cells stall in or undergo a protracted S phase (compare Figure 1O, O' to P, P'). The increase in cells in S phase is coupled with a noticeable absence of cells in mitosis, as revealed by a decrease in cells staining positive for the mitosis marker phosphorylated histone H3 (Figure S1F). Therefore, our data suggest that the eventual loss of germ cells in *mxc* mutant testes results from a failure to maintain GSCs, premature initiation of terminal differentiation, and accumulation of spermatogonia in S-phase, followed by germ cell loss.

Mxc regulates maintenance and differentiation of the somatic lineage in the testis

Somatic cells play an integral role in regulating the behavior of male germ cells in the testis (Kiger et al., 2000; Leatherman and Dinardo, 2008; Leatherman and Dinardo, 2010; Matunis et al., 1997; Tran et al., 2000). Early somatic cyst cells expressing the transcription factor Traffic Jam (TJ) appeared relatively unaffected in testes from males carrying the weakest mxc^{G46} allele (Figure 1E-H). Therefore, we wanted to determine whether *mxc* also regulates

somatic cell behavior, which could contribute to the loss of germ cells observed in *mxc* mutants. To reduce *mxc* expression in CySCs and early cyst cells in adults, we used the bipartite GAL4-UAS system (Brand et al., 1994) in combination with RNAi-mediated knock-down of gene expression. An *mxc*RNAi transgene was expressed under control of the *c587GAL4* driver, and flies were raised at 18°C during development to restrict RNAi transgene expression to adult stages. Upon eclosion (hatching), adult flies were shifted to 29°C to induce expression of *mxc*RNAi in somatic cells surrounding spermatogonia, and knock-down was confirmed by antibody staining (Figure 2A-B').

In flies expressing *mxcRNAi* for 3 days, Tj^+ cyst cells were detected at the testis tip; however, the cyst cells surrounding and in contact with the hub, typically defined as CySCs, were significantly larger when compared to cells found at that position in control testes (Figure 2 B, D-D') (Gonczy and DiNardo, 1996; Leatherman and Dinardo, 2008). After 10 days, a dramatic loss of Tj^+ somatic cells was observed in flies expressing *mxcRNAi* in early cyst cells, when compared to controls (Figure 2 E-F'). Testes also appeared depleted for early germ cells (Figure 2 B-B'), consistent with a loss of CySCs, which play an important role in regulating GSC proliferation. Notably, cyst cells that remain at the tip of the testis after *mxc* depletion express differentiation markers, such as the transcription factor Eyes absent (Eya), which is normally absent from early cyst cells but expressed in differentiated cyst cells that surround spermatocytes (Figure 2 D', F-F"). Therefore, RNAi-mediated depletion of *mxc* in somatic cells revealed that Mxc regulates maintenance and differentiation of both germline and somatic lineages in the testis.

mxc phenotypes are due to excess histone H3

The histone locus body (HLB) is a protein complex responsible for the transcription and 3'end processing of non-polyadenylated histone mRNAs (Marzluff and Duronio, 2002). As a central component of the HLB, Mxc is involved in both transcription and processing of core histone mRNAs (Salzler et al., 2013; White et al., 2011). Quantitative PCR from flies carrying strong (mxc^{G43}) and weak (mxc^{G46}) *mxc* alleles across different developmental stages revealed that histone mRNA levels vary over time and not all histones are affected similarly (Figure 3A and Figure S1A). In general, higher levels of histone H3 and lower levels of histone H1 were observed earliest in the strongest *mxc* mutant backgrounds and at later developmental stages and in mxc^{G46} adults. Eventually, histone mRNA levels decline (Figure 3A), consistent with previously published results (White et al., 2011).

Remarkably, RNAi-mediated knock-down of histone H3 in early germ cells completely suppressed the testis phenotype in mxc^{G46} males (Figure 3B-3E'). The efficiency of H3 RNAi expression was verified using fluorescence *in situ* hybridization (FISH), which showed a distinct reduction of H3 mRNA in early germ cells (Figure S2). The normal gradient of germ cell differentiation and maturation was restored, including maintenance of GSCs (Figure 3F). Moreover, mxc^{G46} males with continuous germline expression of H3 RNAi appear to be as fertile as control flies and give rise to normal progeny (Figure 3G). In contrast to H3, H1 levels were decreased in *mxc* mutants but neither overexpression of histone H1 rescued nor RNAi-mediated knock down of H1 recapitulated *mxc* phenotypes

(Figure S3). Thus, an increase in the levels of histone H3 mRNA appears to be the primary cause of germline loss in *mxc*^{G46} mutant males.

Flies mutant for *mxc* have a classical Polycomb phenotype represented by defects in the specification of sex combs (Santamaría and Randsholt, 1995). Given the suppression of the *mxc* germline phenotype by H3 RNAi, we wanted to determine whether the Polycomb phenotype, ie., ectopic sex combs, could also be rescued by decreasing H3 levels. Sex combs are typically located on the 1st tarsus (T1) of the 1st leg (L1); however, in *mxc*^{G46} males, sex combs are observed on additional legs and tarsi (Figure 3H), indicative of a homeotic transformation of the second and third thoracic segments into the first. In *mxc*^{G46} flies, sex combs were found on the 2nd tarsus (T2) of L1 in 37% of animals examined, while 20% exhibited sex combs on the 2nd leg (L2) and 7% exhibited sex combs on the 3rd leg (L3) (Figure 3H). However, conditional expression of H3 RNAi in imaginal discs of *mxc*^{G46} mutant flies resulted in a significant decrease in the L2 to L1 and L3 to L1 transformations (Figure 3H), suggesting that higher levels of H3 due to *mxc* mutations might compromise the activity of PRCs, resulting in Polycomb phenotypes.

mxc mutant cells accumulate foci of the DNA damage marker γH2Av

Production of new histones is tightly linked to cell cycle progression. Histone synthesis is initiated at the G1/S transition, and new histones are incorporated immediately behind the progressing replication fork during DNA replication. However, excess histones can lead to stalling of the replication fork and present a source of replicative stress and DNA damage (Gunjan and Verreault, 2003; Herrero and Moreno, 2011; Singh et al., 2010) .

Because we observed an accumulation of cells in S phase in the *mxc* mutant background (Figure 1O-O'), we hypothesized that these cells would exhibit hallmarks of replicative stress due to excess H3. Consistent with initiation of a DNA damage response (DDR), foci representing a phosphorylated variant of histone H2A (γH2Av), an early and specific marker of DNA damage, were observed in *mxc* mutant testes (Figure 4A-4C). Indeed, the level of γH2Av observed in germ cells of *mxc*^{G46} mutant testes was similar to the level observed in wild type flies fed the replicative stress-inducing agent hydroxyurea (HU) (Figure 4B, C). In addition, high levels of γH2Av were observed in CySC clones homozygous mutant for *mxc*^{G48} (Figure 4E-E"), suggesting that activation of the DDR correlates with loss of *mxc*.

The DDR appears to be due to the increase in H3, as a decrease in the intensity of γH2Av staining is observed in *mxc*^{G46} mutant germ cells expressing H3 RNAi (Figure 4A, C, D). In addition, GSCs in testes from *mxc*^{G46} males expressing H3 RNAi show fewer γH2Av foci and less intense staining than in *mxc*^{G46} mutant GSCs (Figure 4F, H). In summary, our data suggest that changes in the normal histone mRNA levels, due to *mxc* mutations, induce replicative stress, which can be suppressed by a reduction in histone H3.

Consistent with this model, hallmarks of the *mxc* mutant germ cell phenotype were observed when we induced replicative stress and DNA damage by continuously feeding wild-type flies with HU. In 86% of the testes examined (n=58), loss of early germ cells and the presence of cysts containing less than 16 spermatocytes were observed at the apical tip of the testis (Figure 4 I, J). This implies that loss of stem cells and precocious differentiation

observed in *mxc*^{G46} mutants could be due solely to the replicative stress induced by persistently high H3 levels.

Reduced efficiency of the DNA damage response enhances *mxc* germline phenotypes

At early time points, *mxc*^{G46} mutant germ cells exhibit premature initiation of differentiation, at the expense of continued proliferation (TA divisions) (Figure 1E-G). However, at later time points, cells appear to stall or accumulate in S phase (Figure 1G, I, O) and exhibit hallmarks of a DDR (Figure 4C, E, F), suggesting that cells may exhibit a protracted S phase to attempt DNA repair. Therefore, we hypothesized that abrogating a DDR should enhance the *mxc*^{G46} testis phenotype, which would be represented by an accelerated loss of early germ cells.

Indeed, inhibition of a DDR by mutations in the H2A variant, H2Av, enhanced the *mxc* testis phenotype. H2Av serves as the functional orthologue of both H2Az and H2Ax in mammalian systems (Clarkson et al., 1999; Madigan et al., 2002). Phosphorylation at Ser137 within the C-terminus of *Drosophila* H2Av is one the earliest events in the DDR and is required to enhance DDR efficiency (Madigan et al., 2002). Null mutations in H2Av, such as *H2Av*^{810}, are lethal but viability is rescued by either a wild type transgene or C-terminal deleted version of H2Av (*H2Av*$^{\Delta CT}$) lacking the last 14 amino acids, including Ser137 (Clarkson et al., 1999; Madigan et al., 2002).

Consistent with our prediction, testes from *mxc*^{G46},*H2Av*$^{\Delta CT}$;*H2Av*^{810}/*TM6b* males display an acceleration of the *mxc*^{G46} phenotype, which is now evident in larval (L3) gonads (Figure 5A-C, G). In addition, more than 63% (n=82) of testes from 1do *mxc*^{G46},*H2Av*$^{\Delta CT}$;*H2Av*^{810}/*TM6b* flies exhibit an accumulation of EdU^{+} cells (Figure 5F, F'). Therefore, impairing the efficiency of the DDR extends the time required for *mxc* mutant germ cells to resolve the effects of replicative stress and accelerates the onset of germline phenotypes (compare Figure 1F-1H and Figure 5 A-G).

Reduced efficiency of the DNA damage response enhances Polycomb phenotypes

In addition to enhancing the *mxc* germline phenotype, abrogation of a DDR by mutations in *H2Av* also enhances the presence of ectopic sex combs in *mxc* mutants. Loss of one copy of *H2Av* significantly enhanced the frequency of L2 to L1 and L3 to L1 transformations in *mxc*^{G46} males (Figure 5H). In the presence of the *H2Av*$^{\Delta CT}$ transgene, which rescues viability of *H2Av*^{810} mutant males but cannot be phosphorylated in response to DNA damage, the frequency of L2 to L1 and L3 to L1 transformations was also significantly higher than in the *mxc* mutant background (Figure 5H). Therefore, altering a DDR by blocking phosphorylation of H2Av appears to enhance homeotic transformations typically observed as a consequence of loss of PcG function.

Discussion

Our findings reveal that sustained levels of replicative stress and an ongoing DNA damage response can interfere with maintenance of cell fate decisions and tissue homeostasis. Defects in histone synthesis, resulting in higher histone levels, constitute a pernicious intra-cellular source of replicative stress: it persists while the cells attempt to repair DNA and will

reoccur cyclically in subsequent S phases. Accordingly, an intense DDR is observed both in *mxc* mutant germline and somatic cells (Figure 4). Importantly, induction of replicative stress via another mechanism, ie., continual exposure to hydroxyurea, recapitulated the *mxc* germline phenotypes, including loss of germ cells due to premature initiation of differentiation (Figure 4 I, J). Therefore, we suggest that a widespread and persistent DDR contributes to the precocious initiation of differentiation in *mxc* mutant cells. Due to the degree of EdU incorporation in germ cells within *mxc* mutant testes, we conclude that germ cells undergo a protracted S-phase followed, ultimately, by germ cell loss. However, given the apparent DNA damage in *mxc* mutant cells, it is possible that germ cells are in G2 but continue to incorporate EdU as a consequence of DNA repair. Nonetheless, entry into mitosis is noticeably lacking in *mxc* mutant germ cells, as indicated by an absence of phosphorylated Histone H3 (Figure S1, F, F').

One outstanding question is whether the *mxc* germline and hematopoietic defects described here and elsewhere truly reflect a loss of Polycomb function. Although a role for PcG in regulating stem cell behavior and maintenance of cell identity is well established (Sauvageau and Sauvageau, 2010), a *bona fide* PcG phenotype in the *Drosophila* male germline has not been described previously. Elegant experiments by Chen et al. demonstrated that several PRC1 components are recruited to the nucleolus in spermatocytes upon terminal differentiation, suggesting that PcG activity may be required in early germ cells to repress the expression of differentiation genes (Chen et al., 2005). Interestingly, loss of the *Drosophila* PRC1 members *Psc* [Mel18] and *Su(z)2* [Bmi1] in germ cells did not result in loss of GSCs (Morillo Prado et al., 2012), which may suggest a different PRC1 composition in male germ cells. Moreover, the mammalian homolog of Mxc, NPAT, plays a role in DNA repair by regulating the expression of ATM (Ataxia telangiectasia mutated), in addition to H2 and H4 (Medina et al., 2007; White et al., 2011). Therefore, it is possible that *mxc* plays additional roles in mediating a DNA damage response, which would render *mxc* mutant cells more sensitive to replicative stress.

While mutations in histones have been shown to reproduce or enhance Polycomb phenotypes (Lewis et al., 2013; Pengelly et al., 2013; Swaminathan et al., 2005), to our knowledge, this is the first report of a sustained/hindered DDR enhancing a classical PcG phenotype *in vivo* (Figure 5H). However, it remains unclear how replicative stress and a persistent DDR could influence Polycomb activity, leading to homeotic transformations such as those observed in *mxc* mutants. Recent evidence has implicated PcG proteins in DDR pathways; however, the precise role for PcG proteins in DNA repair has not yet been elucidated. One possibility is that PcG-mediated modification of histones is required for the change in chromatin conformation necessary to allow access of DNA repair machinery to the DNA (Chagraoui et al., 2011; Huertas et al., 2009; Vissers et al., 2012). Alternatively, PcG activity could serve to repress transcription while repair is ongoing (Chagraoui et al., 2011). Both histone H2A and H2Av are mono and polyubiquitinylated during a DDR, including mono-ubiquitination by PRC1 at Lys118 (Vissers et al., 2012). Therefore, an incessant induction of a DDR, such as in the case of *mxc* mutation, could result in persistent, high levels of ubiquitination at sites of DNA repair, which may interfere with the normal dynamic of mono-ubiquitination/deubiquitination of H2Av on Lys118 necessary for PcG-

mediated repression (Scheuermann et al., 2010). On the other hand, a persistent DDR could alter PcG activity by recruiting PcG proteins to sites of DNA damage and away from normal target genes that regulate cellular identity and cell fate decisions. Regardless of whether PcG proteins play an active role in DNA repair, our data provide evidence *in vivo* that Polycomb activity can be influenced by persistent DNA damage. Therefore, we propose that any moderate, continuous source of replicative stress during development and/or in adult stem cell lineages could trigger aberrant gene expression and alterations in cell fate decisions.

Materials and Methods

Drosophila stocks and husbandry

Flies were raised at 25°C on standard cornmeal-molasses agar medium. All *mxc* alleles (w^1 mxc^{G43}/*FM7c*, y^1 ac^1 mxc^{G48}/*FM7a* and w^1 mxc^{G46}/*FM7a*), stocks for clonal analysis (Tft^1 *P{neoFRT}40A/CyO*), RNAi mediated depletion (*H3* RNAi: y[1] sc[*] v[1]; P{y[+t7.7] v[+t1.8]=TRiP.GL00255}attP2, H1 RNAi: y^1 *sc* v*^{1}*; P{TRiP.GL00081}attP2, GAL4* RNAi: y[1] sc[*] v[1]; P{y[+t7.7] v[+t1.8]=VALIUM20-GAL4.1}attP2), stock carrying *P{tubP-GAL80[ts]}7, P{tub-GAL4}1* and the *w*; P{GAL4-wg.M}MA1* stock were obtained from the Bloomington stock center. Experiments involving mxc^{G46} adults were performed on testes from mxc^{G46} male progeny from mxc^{G46}/*FM7a* females outcrossed to w^{1118} males. Male mxc^{G43} or mxc^{G46} mutant larvae were selected from mxc^{G43}/*FM7c, Kr-GAL4, UAS-GFP* or mxc^{G46}/*FM7c, Kr-GAL4, UAS-GFP* stocks based on the absence of GFP expression (Casso et al., 2000). The *c587GAL4* driver line was a gift from Ting Xie, and the *nanosGAL4:VP16, UAS-GFP* driver was initially described in Van Doren et al., 1998.

Stocks carrying *Sa::GFP* (Chen et al., 2005) and *Myc::Can* (Hiller et al., 2001) tagged proteins were generously provided by Xin Chen and Margaret Fuller, respectively. The mxc^{G48}, *Sa::GFP* line was generated by recombining the *Sa::GFP* transgene and mxc^{G48} allele onto the same X chromosome. Control flies, when not otherwise specified, were from an isogenized w^{1118} stock provided by D. Walker.

Stocks carrying the X-linked $H2Av^{\Delta CT}$ transgene was generated by Clarkson *et al* (Clarkson et al., 1999), and flies were kindly provided by Yikang Rong. The stock $H2Av^{\Delta CT}$;$H2av^{810}$/*TM6Ubx* was generated using the Bloomington stock *w*; His2Av*^{810}*/TM3,Sb*^{1}. Flies of the genotype $H2Av^{\Delta CT}$;$H2av^{810}$/$H2av^{810}$ were frequently observed, validating that the *H2Av* rescues viability of the $H2av^{810}$/$H2av^{810}$ mutants. The $H2Av^{\Delta CT}$ transgene was recombined with the mxc^{G46} allele onto the same X chromosome to generate mxc^{G46}, $H2Av^{\Delta CT}$ flies. In contrast to $H2Av^{\Delta CT}$;$H2av^{810}$/$H2av^{810}$ flies, mxc^{G46}, $H2Av^{\Delta CT}$;$H2av^{810}$/$H2av^{810}$ flies are not viable. Therefore, experiments were conducted using mxc^{G46}, $H2Av^{\Delta CT}$;$H2av^{810}$/*TM6b* flies.

A stock carrying the heat-shock inducible H3.3::GFP was generously provided by Kami Ahmad (Ahmad and Henikoff, 2002).

Generation of *mxc::GFP* transgenic flies

The *mxc::GFP* transgene was generated as follows: the entire *mxc* (*CG12124*) coding region (including introns) in addition to 625 bp upstream of the *mxc* start codon, (promoter region

between *mxc* and *dLarp7/CG42569*) were PCR amplified and cloned in frame with GFP into the phiC31-based transformation vector pattB (a gift from Johannes Bischof, Basler lab, Zurich). The GFP open reading frame was inserted between the last *mxc* codon before the stop codon (TGA) and the *mxc* 3'UTR. DNA was sent for injection to Genetic Services, Inc (MA, USA). The phiC31 system was used with the attp40 landing site on the second chromosome. Three lines were obtained, and all three exhibited the same GFP staining pattern for Mxc::GFP.

Fertility test

Single 1-2do male progeny from w^{1118} stocks (control) or mxc^{G46}*;nanosG4>Gal4RNAi* or mxc^{G46}*;nanosG4>H3RNAi* crosses were mated to 3 w^{1118} virgin females (30 males total for each genotype) at 25°C. Parents were removed from the vials 4 days later, and adult progeny were counted 10 days after the crosses were established. The experiment was performed in duplicate : males used initially were crossed again 5 days later to new virgin females. Statistical significance of the results was determined using Graphpad Prism, and after evaluation of the normality of the values, the Kruskal-Wallis test was applied. Both experiments (with 1-2do males or 5 do males) gave the same result.

Clonal analysis

For clonal analysis, the *mxc::GFP* transgene was recombined onto the *FRT40A* chromosome (carrying a neomycin resistance gene), and a mxc^{48}*/FM7; mxc::GFPFRT40A/CyO* stock was generated. Those females were crossed to *FRT40A/CyO; hsFLP/MKRS* males, and viable mxc^{48}*/Y; mxc::GFP-FRT40A/FRT40A; hsFLP/+* males were recovered. Those males were heat-shocked twice a day (morning and evening) for 2 days during 30 min at 37°C in a circulating water bath and maintained at room temperature (22-23°C) between heat-shocks. Clone induction was visualized by loss of the Mxc::GFP nuclear body in $Vasa^{+}$ germ cells (GSCs) or Tj^{+} cells adjacent to the hub (CySCs). To address GSC maintenance, testes were dissected after 3 or 10 days post heat-shock. The number of testes with at least one GFP^{-} GSC was used as a read-out of clone induction and GSC maintenance.

RNAi-mediated knock down of gene expression

Specific depletion of *mxc* from cyst cells was obtained using an *mxc* RNAi line from the Harvard TRiP stock collection ($mxc^{JF01992}$, BL25970) expressed under the control of the cyst cell driver *c587GAL4* in combination with $GAL80^{ts}$ to repress GAL4 activity. The *GAL4* RNAi TRiP line (BL35784) was used as a negative control. The flies were maintained at 18-20°C until pupariation and were shifted to 29°C to activate RNAi expression until eclosion. Similar results were obtained using an independent *mxc* RNAi line from VDRC (v42978) expressed with *c587GAL4.* For these experiments, flies were raised and maintained at 25°C.

Reduction of H3 and H1 in the germ line of mxc^{G46} males was achieved using the H3 RNAi TRiP lines expressed under the control of the *nanosGAL4:VP16, UAS-GFP* driver (Van Doren et al., 1998), and the *GAL4* RNAi line (BL35784) was used as a negative control. Conditional expression of H3 RNAi to target sex combs specification during development

was achieved by crossing *mxc^{G46}; Wingless-GAL4/TM6Ubx* females to *GAL80^{ts}/CYO;H3RNAi* or *GAL4RNAi* males.

EdU incorporation experiments

EdU incorporation was done using the Click-iT EdU Imaging kit (Invitrogen) according to manufacturer instructions. Briefly, testes were dissected in 1X Ringer's buffer (NaCl 155mM, KCl 5mM, $CaCl_2$ 2mM, $MgCl_2$ 1mM, NaH_2PO_4 2mM, HEPES 10mM, Glucose 10mM) and incubated in a 30μM EdU/1X Ringer's buffer solution during 30 min. Testes were fixed 20min in 4% formaldehyde, washed twice 5min in 3%BSA/1XPBS, and incubated 20min in 1X PBS-0.5% Triton X-100 (PBST). Testes were next incubated 30min with the Click-iT reaction cocktail, rinse and subsequently blocked in 3% BSA/PBST. Samples were then subjected to the regular IF protocol.

Hydroxyurea treatment

For accute treatment with hydroxyurea (HU), flies were starved for 8 hours before being exposed overnight to a regular vial of fly food containing a Kimwipe soaked in a grape juice-10mg/mL HU solution. Testes were dissected 16h later. For the prolonged exposure to HU, flies were maintained at 25°C for 5 days in a vial of fly food mixed with 3mg/mL HU.

Immunofluorescence and microscopy

Immunofluorescence (IF) was performed on whole-mount testes dissected in PBS and fixed in 2% PFA as previously described (Boyle et al., 2007).

Antibodies used were: rabbit anti-Vasa (1:5000, a gift from P. Lasko); mouse anti-Fas3 (7G10)(1:20), rat anti-DEcadherin (DCAD2)(1:20), mouse anti-Myc 9E10 (1:50) obtained from the Developmental Studies Hybridoma Bank developed under the auspices of the National Institute of Child Health and Human Development and maintained by the University of lowa; guinea pig anti-traffic jam (Tj) (1:3000, a gift from D. Godt), rabbit anti-FLASH (1:1000) and rabbit anti-Mxc (1:1000) (gift from W. Marzluff), rabbit anti-GFP (1:5000, Invitrogen); rabbit H2AvD pS137 antibody (anti-γH2Av, 1:1000, Rockland), mouse anti-pHH3 (1:400, Cell Signaling), rabbit anti-H1 (Drosophila specific, 1:1000, Active Motif). Tissues were mounted in Vectashield with DAPI (Vector Laboratories). Secondary antibodies were obtained from Invitrogen and used 1:400.

Mounting of legs to quantify sex combs was performed as follows: fly legs were dissected in 1X PBS and boiled 10min in 10% KOH. Samples were washed twice with water, and twice with 100% ethanol. A mix of lactic acid /ethanol (6/5) was added and the legs were mounted on slides.

Phase contrast images of squashed testes and fly legs were obtained using a Leica DM5000 microscope equipped with a DC500 camera using Firecam imaging software (version 1.7.1; Leica Microsystems). All other images were obtained using a Zeiss LSM 710/780 Laser Scanning confocal microscope. All experiments involving cell counts and pixel quantification were performed using multiple sections (Z-stacks) from confocal images.

Image processing, area measurement and pixel quantification were executed with ImageJ 1.45r (Wayne Rasband, National Institute of Health, http://imagej.nih.gov/ij).

Fluorescent In Situ Hybridization (FISH)

Performed as described in Toledano et al. (Toledano et al., 2012). The entire open reading frame of the histone H3 gene was used as a probe.

Quantitative real-time PCR

RNA was extracted using TRizol (Invitrogen) according to manufacturer's instructions. After DNAse treatment (RQ1, Promega), RNA was quantified and 300ng were used in each reverse transcription reaction (Superscript III First Strand, Invitrogen). For the PCR reaction, 1/12 of cDNA, 0.2μM primers, and 1X SYBR Green mix (Applied Biosystem) were used with the following cycle in a ABI Prism cycler: 10min 95°C, (15 sec 95°C, 45sec 60°C) 39X. The primers used were as follows: H1-f (5'GCA AAA GCC AAG GAT GCC AAG AAA ACT G3'), H1-r (5'ACT TTT TGG CAG CCG TAG TCT TCG3'), H2A-f (5'GCT GGC AAT GCT GCT CGT GAC AA3'), H2A-r (5'AGG CCT TCT TCT CGG TCT TCT TG3'), H2B-f (5'GAA GGC GAT GAG CAT AAT GAA CAG CT3'), H2B-r (5'ATT TAG AGC TGG TGT ACT TGG TGA C3'), H3-f (5'AGA CGG ACT TGC GAT TCC AGA GC T3'), H3-r (5'AAG CAC GCT CGC CGC GAA TG 3'), H4-f (5'GCG GTG TGA AGC GCA TAT CTG GA3'), H4-r (5'AAC CGC CAA ATC CGT AGA GGG T3'), GAPDH-f (5'GCG GTA GAA TGG GGT GAG AC3'), GAPDH-r (5'TGA AGA GCG AAA ACA GTA GC3'). Each sample was duplicated on the PCR plate, and the final results average 3 biological replicates. For the quantification, the comparative C_T method was used after the primers efficiency was verified and validated in a plot of log input amount versus ΔC_T.

Statistical analysis

All quantitative experiments were evaluated for statistic significance using the software Graphpad prism, after verifying the normality of values and equivalence of variances. For the qRT-PCR, each sample was duplicated on the PCR plate, and the final results average the $\Delta\Delta C_T$ of 3 biological replicates. The statistical significance of observed differences in the fold changes was tested against a theoretical mean equal to 1 in a one sample Students t-test. For stem cell counts and pixel quantification, the statistical differences between mutant or RNAi-treated samples and controls were addressed using a Students two-tailed t-test. For the sex combs phenotype on male legs, results were translated into individual contingency tables for each legs, where each row defines a genetic background (for example mxc^{G46},$H2Av^{WT}$ versus mxc^{G46},$H2Av^{\Delta CT}$), each column defines an outcome (normal leg or leg with misplaced sex combs) and each value is an exact count. Statistical significance was assayed using a two-sided Chi-square test. Statistical significance was concluded whenever the calculated $P < 0.05$.

Acknowledgments

We are grateful to P. Lasko, D. Godt, R. Glaser for generous gifts of antibodies, M. Fuller, X. Chen, Y. Rong and K. Ahmad for sharing flies stocks, N. Randsholt for information regarding *mxc* alleles, R. Duronio and W. Marzluff for sharing reagents, fly stocks, and data prior to publication, and Jonah Cool and members of the Jones lab who

contributed to constructive discussions. We thank the TRiP at Harvard Medical School (NIH/NIGMS R01-GM084947) for providing transgenic RNAi fly stocks used in this study, and the Bloomington stock center. This work was supported by a Pioneer Award from the Salk Institute (S.L.), and the G. Harold and Leila Y. Mathers Charitable Foundation, the American Federation for Aging Research, the California Institute for Regenerative Medicine, and the NIH (D.L.J).

References

Ahmad K, Henikoff S. The histone variant H3.3 marks active chromatin by replication-independent nucleosome assembly. Mol. Cell. 2002; 9:1191–1200. [PubMed: 12086617]

Becker KA, Ghule PN, Lian JB, Stein JL, van Wijnen AJ, Stein GS. Cyclin D2 and the CDK substrate p220(NPAT) are required for self-renewal of human embryonic stem cells. J. Cell. Physiol. 2010; 222:456–464. [PubMed: 19890848]

Boyle M, Wong C, Rocha M, Jones DL. Decline in self-renewal factors contributes to aging of the stem cell niche in the Drosophila testis. Cell Stem Cell. 2007; 1:470–478. [PubMed: 18371382]

Casso D, Ramírez-Weber F, Kornberg TB. GFP-tagged balancer chromosomes for Drosophila melanogaster. Mech. Dev. 2000; 91:451–454. [PubMed: 10704882]

Chagraoui J, Hébert J, Girard S, Sauvageau G. An anticlastogenic function for the Polycomb Group gene Bmi1. Proc. Natl. Acad. Sci. U.S.A. 2011; 108:5284–5289. [PubMed: 21402923]

Chen X, Hiller M, Sancak Y, Fuller MT. Tissue-Specific TAFs Counteract Polycomb to Turn on Terminal Differentiation. Science. 2005:1–5.

Clarkson MJ, Wells JR, Gibson F, Saint R, Tremethick DJ. Regions of variant histone His2AvD required for Drosophila development. Nature. 1999; 399:694–697. [PubMed: 10385122]

Docquier F, Saget O, Forquignon F, Randsholt NB, Santamaria P. The multi sex combs gene of Drosophila melanogaster is required for proliferation of the germline. Development Genes and Evolution. 1996; 205:203–214.

Van Doren M, Williamson AL, Lehmann R. Regulation of zygotic gene expression in Drosophila primordial germ cells. Curr. Biol. 1998; 8:243–246. [PubMed: 9501989]

Fuller M. Bate M, Martinez-Arias A. Spermatogenesis. The Development of Drosophila. 1993

Ghule PN, Dominski Z, Yang X-C, Marzluff WF, Becker KA, Harper JW, Lian JB, Stein JL, van Wijnen AJ, Stein GS. Staged assembly of histone gene expression machinery at subnuclear foci in the abbreviated cell cycle of human embryonic stem cells. Proc. Natl. Acad. Sci. U.S.A. 2008; 105:16964–16969. [PubMed: 18957539]

Gunjan A, Verreault A. A Rad53 Kinase-Dependent Surveillance Mechanism that Regulates Histone Protein Levels in S. cerevisiae. Cell. 2003; 115:537–549. [PubMed: 14651846]

Herrero AB, Moreno S. Lsm1 promotes genomic stability by controlling histone mRNA decay. EMBO J. 2011; 30:2008–2018. [PubMed: 21487390]

Hiller MA, Lin TY, Wood C, Fuller MT. Developmental regulation of transcription by a tissue-specific TAF homolog. Genes Dev. 2001; 15:1021–1030. [PubMed: 11316795]

Kiger AA, Jones DL, Schulz C, Rogers MB, Fuller MT. Stem cell self-renewal specified by JAK-STAT activation in response to a support cell cue. Science. 2001; 294:2542–2545. [PubMed: 11752574]

Leatherman JL, Dinardo S. Germline self-renewal requires cyst stem cells and stat regulates niche adhesion in Drosophila testes. Nat Cell Biol. 2010

Lewis EB. A gene complex controlling segmentation in Drosophila. Nature. 1978; 276:565–570. [PubMed: 103000]

Lewis PW, Müller MM, Koletsky MS, Cordero F, Lin S, Banaszynski LA, Garcia BA, Muir TW, Becher OJ, Allis CD. Inhibition of PRC2 activity by a gain-of-function H3 mutation found in pediatric glioblastoma. Science. 2013; 340:857–861. [PubMed: 23539183]

Madigan JP, Chotkowski HL, Glaser RL. DNA double-strand break- induced phosphorylation of Drosophila histone variant H2Av helps prevent radiation-induced apoptosis. Nucleic Acids Res. 2002; 30:3698–3705. [PubMed: 12202754]

Marzluff W, Duronio R. Histone mRNA expression: multiple levels of cell cycle regulation and important developmental consequences. Current Opinion in Cell Biology. 2002; 14:692–699. [PubMed: 12473341]

Medina R, van der Deen M, Miele-Chamberland A, Xie R-L, van Wijnen AJ, Stein JL, Stein GS. The HiNF-P/p220NPAT Cell Cycle Signaling Pathway Controls Nonhistone Target Genes. Cancer Research. 2007; 67:10334–10342. [PubMed: 17974976]

Morillo Prado JR, Chen X, Fuller MT. Polycomb group genes Psc and Su(z)2 maintain somatic stem cell identity and activity in Drosophila. PLoS ONE. 2012; 7:e52892. [PubMed: 23285219]

Pengelly AR, Copur Ö, Jäckle H, Herzig A, Müller J. A histone mutant reproduces the phenotype caused by loss of histone-modifying factor Polycomb. Science. 2013; 339:698–699. [PubMed: 23393264]

Saget O, Forquignon F, Santamaria P, Randsholt NB. Needs and targets for the multi sex combs gene product in Drosophila melanogaster. Genetics. 1998; 149:1823–1838. [PubMed: 9691040]

Salzler HR, Tatomer DC, Malek PY, McDaniel SL, Orlando AN, Marzluff WF, Duronio RJ. A sequence in the Drosophila H3-H4 Promoter triggers histone locus body assembly and biosynthesis of replication-coupled histone mRNAs. Dev. Cell. 2013; 24:623–634. [PubMed: 23537633]

Santamaria FDOSFFNBR. The multi sex combs gene of Drosophila melanogaster is required for proliferation of the germline. Roux's Arch Dev Biol. 1995:1–12.

Santamaría P, Randsholt NB. Characterization of a region of the X chromosome of Drosophila including multi sex combs (mxc), a Polycomb group gene which also functions as a tumour suppressor. Mol. Gen. Genet. 1995; 246:282–290. [PubMed: 7854313]

Sauvageau M, Sauvageau G. Polycomb group proteins: multi-faceted regulators of somatic stem cells and cancer. Cell Stem Cell. 2010; 7:299–313. [PubMed: 20804967]

Scheuermann JC, de Ayala Alonso AG, Oktaba K, Ly-Hartig N, McGinty RK, Fraterman S, Wilm M, Muir TW, Müller J. Histone H2A deubiquitinase activity of the Polycomb repressive complex PR-DUB. Nature. 2010; 465:243–247. [PubMed: 20436459]

Schwartz YB, Pirrotta V. Polycomb silencing mechanisms and the management of genomic programmes. Nat. Rev. Genet. 2007; 8:9–22. [PubMed: 17173055]

Singh RK, Liang D, Gajjalaiahvari UR, Kabbaj M-HM, Paik J, Gunjan A. Excess histone levels mediate cytotoxicity via multiple mechanisms. Cell Cycle. 2010; 9:4236–4244. [PubMed: 20948314]

Sparmann A, Lohuizen M. van. Polycomb silencers control cell fate, development and cancer. Nat Rev Cancer. 2006; 6:846–856. [PubMed: 17060944]

Swaminathan J, Baxter EM, Corces VG. The role of histone H2Av variant replacement and histone H4 acetylation in the establishment of Drosophila heterochromatin. Genes Dev. 2005; 19:65–76. [PubMed: 15630020]

Toledano H, D'Alterio C, Loza-Coll M, Jones DL. Dual fluorescence detection of protein and RNA in Drosophila tissues. Nat Protoc. 2012; 7:1808–1817. [PubMed: 22976352]

Tulina N, Matunis E. Control of stem cell self-renewal in Drosophila spermatogenesis by JAK-STAT signaling. Science. 2001; 294:2546–2549. [PubMed: 11752575]

Vissers JHA, van Lohuizen M, Citterio E. The emerging role of Polycomb repressors in the response to DNA damage. J. Cell. Sci. 2012; 125:3939–3948. [PubMed: 23104738]

White AE, Burch BD, Yang X-C, Gasdaska PY, Dominski Z, Marzluff WF, Duronio RJ. Drosophila histone locus bodies form by hierarchical recruitment of components. J Cell Biol. 2011; 193:677–694. [PubMed: 21576393]

Xu T, Rubin GM. Analysis of genetic mosaics in developing and adult Drosophila tissues. Development. 1993; 117:1223–1237. [PubMed: 8404527]

Highlights

- Mutations in *multi sex combs* (*mxc*) disrupt male germline homeostasis
- Mutations in *mxc* result in high levels of histone H3 and replicative stress
- Exposure to hydroxyurea mimics *mxc* mutant phenotypes in the testis
- An altered DNA damage response enhances *mxc* mutant phenotypes

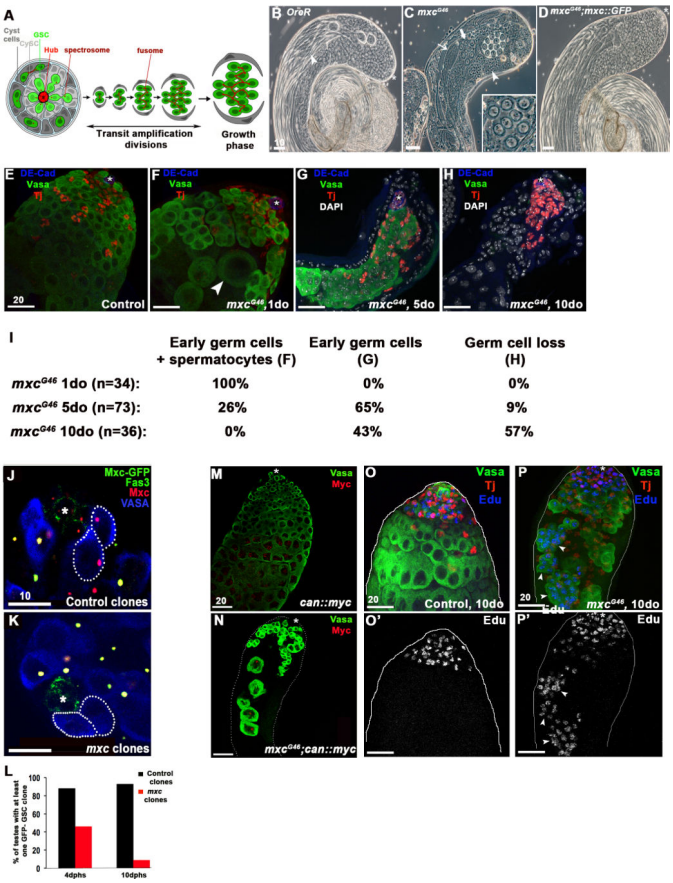

Figure 1. Mutations in *mxc* result in germ cell loss over time

A. Schematic of *Drosophila* spermatogenesis. GSC: germline stem cell; CySC: cyst stem cell. **B.** Phase contrast image of a normal testis showing the spatial gradient of germ cell development. GSCs and spermatogonia are located at the tip (asterisk), followed by spermatocytes cysts in growth phase, meiotic germ cells, haploid spermatids and mature sperm, visable in the lumen of the testis (arrowhead). **C.** Testes mutant for mxc^{G46} show loss of germ cells but differentiated cell types are present (spermatid cyst at onion stage, arrowhead; spermatocytes, thick arrow; elongating spermatids, thin arrow). Cysts of <16 germ cells are often observed (inset). **D.** The mxc^{G46} testis phenotype is completely rescued by a *mxc::GFP* transgene. **E.** Control testis filled with Vasa+ germ cells (green), Traffic-Jam^{+} (Tj^{+}) somatic cyst cells (red), and hub cells (asterisk) expressing DE-Cad^{+} (blue). **F.** mxc^{G46} testis contains large spermatocytes (arrowhead) intermingled with spermatogonia and early spermatocyte cysts. **G.** mxc^{G46} testis containing spermatogonia and cyst support cells only. Note absence of spermatocytes. **H.** mxc^{G46} testis completely devoid of germ cells. **I.** Table representing increasing severity of mxc^{G46} testes phenotype over time (1 to 10 days old). **J.** Control GSC clones (Vasa^{+}, blue, dashed lines) around the hub (Fas3^{+}, green, asterisk), induced by FRT-mediated loss of an *mxc::GFP* rescue transgene, still express endogenous Mxc (red). **K.** GSC clones homozygous mutant for mxc^{G48} do not express *mxc::GFP* nor endogenous Mxc (as shown by the loss of Mxc nuclear body). **L.** mxc^{G48} mutant GSCs are lost over time, while control GSC clones are maintained 10 days post heat shock (dphs). **M-N:** Large mxc^{G46} mutant germ cells express the spermatocyte marker

cannonball (*can*) (Myc^{+}, red, arrowhead). **O-O':** EdU incorporation is limited to actively dividing spermatogonia in the transit amplifying (TA) region at the tip of the testis in controls. Germ cells, green (Vasa^{+}), cyst cells, red (Tj^{+}), EdU, blue. **P-P' :** *mxc*^{G46} mutant testis containing spermatogonia (Vasa^{+}, green) in S-phase, indicated by EdU incorporation in germ cell cysts outside of the mitotic zone (arrowheads). Scale bars indicated in μM.

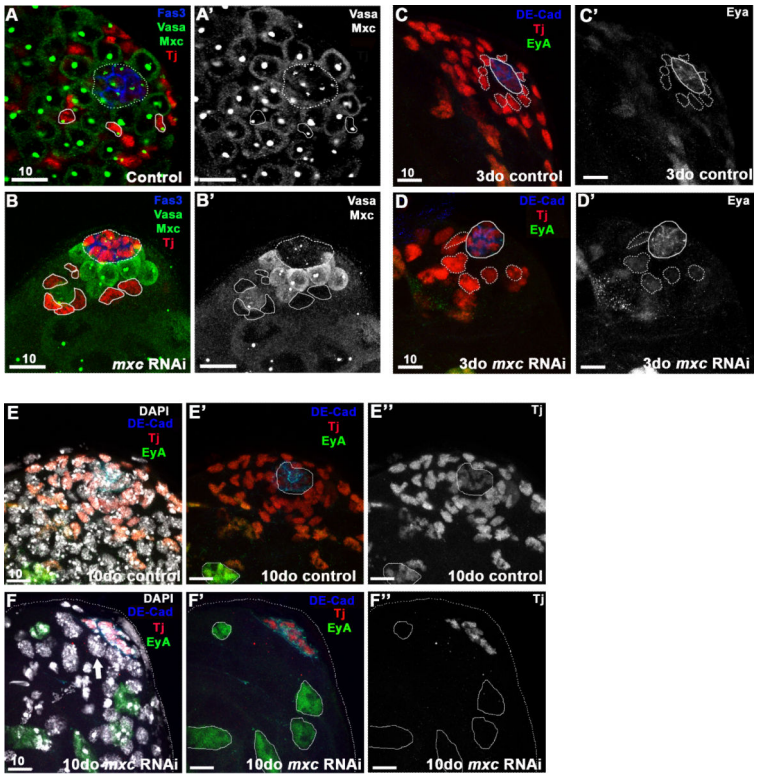

Figure 2. A-D' : Mxc is required autonomously for maintenance of early cyst cells

RNAi-mediated knock-down of *mxc* (RNAi induced for 7d) in early cyst cells (Tj^+, red) using the *c587GAL4* driver results in a significant reduction in cyst cells at the testis tip, including CySCs (**B**), when compared to controls (**A**). Loss of Mxc staining in cyst cells (circled, **B-B'** compared to **A-A'**) confirmed efficiency of RNAi-mediated knockdown. Germ cells (Vasa, green), Mxc (HLB, green), and hub (Fas3, blue; dashed circle). **C-D** The nuclei of Tj^+ cells adjacent to the hub (CySCs, dotted line) are significantly larger 3 days after induction of *mxc*RNAi **(D, D')** when compared to controls (**C, C'**) and express higher levels of the late cyst cell marker Eyes absent (Eya, green), indicating precocious differentiation. Early cyst cells (Tj^+, red), hub ($DE\text{-}cad^+$, blue), late cyst cells (Eya^+, green). **E-F"** : Ten days after induction of *mxc*RNAi, late cyst cells (EyA^+/Tj^-, green) replace early cyst cells (Tj^+, red) at the apical tip (**F-F"**). DAPI staining in **F** reveals the presence of germ cells (Tj^-, EyA^-) at the tip of the testis, adjacent to the hub (thick arrow), similar to **B.** Scale bars indicated in μM.

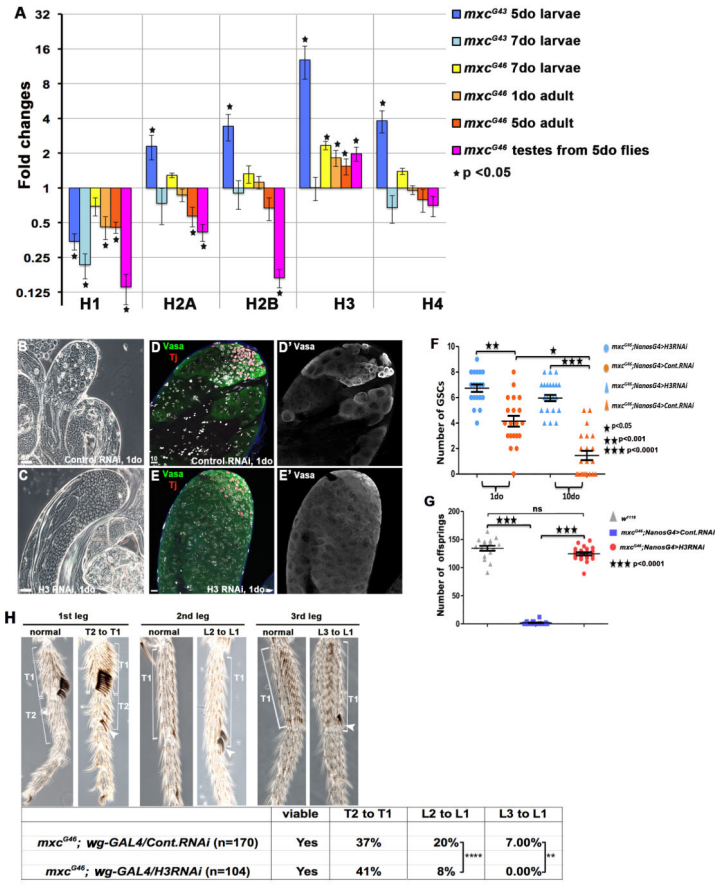

	viable	T2 to T1	L2 to L1	L3 to L1
mxc^{G46}; *wg-GAL4/Cont.RNAi* (n=170)	Yes	37%	20%	7.00%
mxc^{G46}; *wg-GAL4/H3RNAi* (n=104)	Yes	41%	8%	0.00%

Figure 3. Loss of germ cells in *mxc* mutants is rescued by RNAi-mediated depletion of Histone H3

A. Quantitative real time PCR of histone levels in an *mxc* allelic series throughout development, performed on either whole larvae, whole adults or dissected testes. Controls were w^{1118} flies. Significant, fold changes (*mxc* mutant/control) are indicated by asterisks. **B-E'**: The *mxc*^{G46} testis phenotype is suppressed by specific expression of H3 RNAi in early germ cells (**C, E-E'**), in comparison to expression of a control RNAi line (*GAL4*) (**B, D-D'**) Germ cells (Vasa^{+}, green); cyst cells (Tj^{+}, red). The loss of GSCs is rescued in *mxc*^{G46} mutant testes expressing H3 RNAi in early germ cells (**F**), and the fertility of *mxc*^{G46} mutant males expressing H3 RNAi is restored (**G**). Scale bars indicated in μM. **H**: In wild-type males, sex combs are positioned on the 1st tarsus (T1) of the first leg (L1), but ectopic sex combs appear on T2 of L1, T1 of L2 and T1 of L3 of *mxc*^{G46} males, resulting in partial transformations of T2 to T1, L2 to L1 and L3 to L1, respectively. Conditional expression of H3 RNAi during development reduces the L2 to L1 and L3 to L1 transformations (Table).

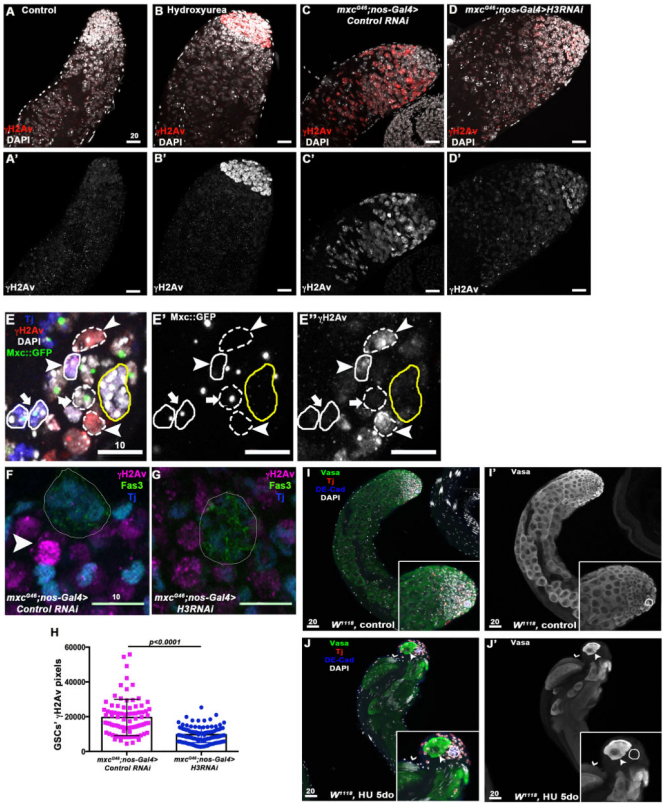

Figure 4. Persistent replicative stress leads to premature differentiation and germline loss.

A-B'. Little to no staining for γH2Av is observed in control testes (**A-A'**). Hydroxyurea treatment induces replicative stress in mitotic germ cells leading to accumulation of γH2Av (red) at the testis tip (**B-B'**). **C-D'** Intense staining for γH2Av is observed in testes from *mxc*^{G46} males (**C-C'**), which is reduced upon H3 RNAi expression in early germ cells (**D-D'**). (**E-E")** Clone induction in the testis using the null mutant allele of *mxc*, *mxc*^{G48}. The Tj^{+} cell (blue) adjacent to the hub (yellow circle) circled by a solid line and indicated by an arrowhead represents a CySC mutant for *mxc* (as shown by the loss of Mxc ::GFP, **E'**) with high level of γH2Av in comparison to wild-type cyst cells (solid circle, arrow, **E"**). As expected, *mxc*^{G48} mutant germ cell clones (dashed line, arrowhead) also express high level of γH2Av compared to wild-type germ cells (dashed line, arrow). **F-H**. *mxc* mutant GSCs display saturation of γH2Av staining (magenta, **F**, arrowhead), which is less frequent and intense upon RNAi-medited reduction in H3 (**G**) Cyst cells (Tj^{+}, blue); hub (Fas3^{+}, green). The levels of γH2Av are significantly reduced in GSCs expressing H3 RNAi (**H**). **I-J'** Prolonged exposure to hydroxyurea recapitulates *mxc* phenotypes. (**I-I"**) Testes from control flies contain early germ cells (Vasa^{+}, green) at the tip (hub is circled, DE-Cad^{+}, blue) followed by growing spermatocytes. (**J-J')** Wild-type flies fed hydroxyurea for 5 consecutive days are depleted for early germ cells and contain cysts with fewer than 16 cells (arrowhead) close to the hub (circled), indicating incomplete TA divisions and precocious differentiation. Germ cells undergoing terminal differentiation are also present at the tip of the testes, as shown by cysts of elongating spermatids (thin arrowhead). Scale bars are in μM.

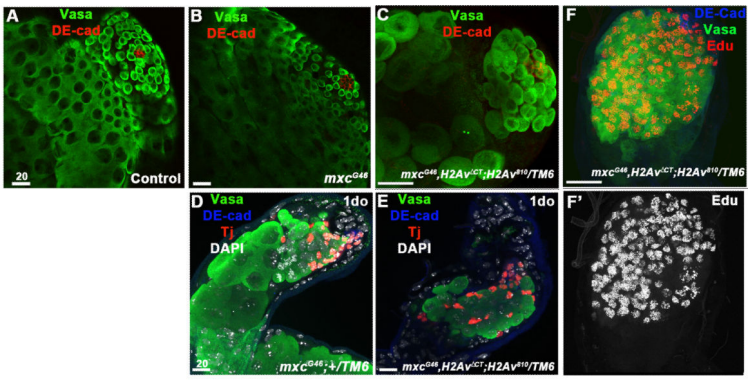

G

		Early germ cells + spermatocytes (D)	Early germ cells (E)	Germ cell loss
mxc^{G46};+/TM6	(n=32) :	100%	0%	0%
mxc^{G46},$H2Av^{\Delta CT}$;$H2Av^{810}$/TM6	(n=82) :	6%	13%	81%

H

	viable	T2 to T1	L2 to L1	L3 to L1
mxc^{G46}; +/TM6 (n=128)	Yes	31%	35%	2.50%
mxc^{G46}; $H2Av^{810}$/TM6 (n=114)	Yes	25%	**** 54%	**** 40%
mxc^{G46}, $H2Av^{\Delta CT}$; $H2Av^{810}$/TM6 (n=222)	Yes	31%	45%	17%

**** p<0.0001

Figure 5. Mutations in *H2Av* enhance the onset of *mxc* germline phenotypes and ectopic sex combs

A-D. Male gonads from (**A**) wild-type and (**B**) mxc^{G46} 3rd instar larvae appear wild-type, while the *mxc* mutant phenotype is detected at this stage in mxc^{G46},$H2Av^{\Delta CT}$;$H2Av^{810}$/ TM6b (**C**) male larvae. Germ cells ($Vasa^+$, green); hub ($DE\text{-}cad^+$, red). **(D, G)** Testes from 1-day old mxc^{G46} adults, exhibit a combination of early germ cells and large germ cells that have initiated differentiaiton prematurely. Germ cells ($Vasa^+$, green); hub ($DE\text{-}cad^+$, blue); cyst cells (Tj^+, red). (**E, F, G**) Testes from 1-day old mxc^{G46},$H2Av^{\Delta CT}$; $H2Av^{810}$/TM6b flies accumulate spermatogonia that appear to be stalled in S-phase, as indicated by EdU incorporation. (**H**) The L2 to L1 and L3 to L1 transformations are enhanced in mxc^{G46} ;$H2Av^{810}$/TMb and mxc^{G46}, $H2Av^{\Delta CT}$;$H2Av^{810}$/TM6b flies.